Eur. Phys. J. B **6**, 459–466 (1998)

THE EUROPEAN PHYSICAL JOURNAL B

Magnetic properties of small Yttrium clusters

R. Guirado-López[1], D. Spanjaard[1,a], and M.-C. Desjonquères[2,b]

[1] Laboratoire de Physique des Solides, Université Paris-Sud, Bâtiment 510, 91405 Orsay, France
[2] Service de Recherche sur les Surfaces et l'Irradiation de la Matière, CE-Saclay, 91191 Gif-sur-Yvette, France

Received: 27 April 1998 / Received in final form: 23 June 1998 / Accepted: 17 July 1998

Abstract. The magnetic properties of small Y_N clusters are studied by using a tight-binding Hubbard Hamiltonian in the unrestricted Hartree-Fock approximation. Several types of cluster geometries are considered in order to see the effects of the size and symmetry of the structures on the magnetic properties. The average magnetic moments $\langle M \rangle$ are found to be constant over large domains of variations in the interatomic distance, a fact that can be explained by the existing closed shell electronic configurations at least for one spin direction in all our magnetic solutions. Small energy gains upon the onset of magnetization are obtained, which reveals the low stability of the magnetic solutions. Our results contradict the prediction of a magnetic-nonmagnetic transition at a large cluster size (about 90 atoms) for these kinds of systems.

PACS. 36.40.Cg Electronic and magnetic properties of clusters – 61.46.+w Clusters, nanoparticles, and nanocrystalline materials

1 Introduction

The study of the magnetic properties on free transition metal (TM) clusters has motivated a remarkable research activity in the past years. In these kinds of systems, the lowered dimensionality and coordination number, as well as high symmetry, are expected to produce nonzero magnetization in clusters for which bulk materials are nonmagnetic or enhanced magnetic moments when the bulk counterpart is already magnetic. In the 3*d* TM series, experimental [1–3] and theoretical [4–7] calculations yielded average magnetic moments increased with respect to their bulk values. In the 4*d* series Cox and co-workers [8] have found that Rhodium clusters exhibit spontaneous magnetization, which was the first case where a nonmagnetic solid has been shown to be magnetic as a cluster. Theory [9–11] and experiments [8] also agree in the existence of magnetic order in Ru and Pd clusters, although discrepancies exist in the magnitude of the total moments. Such differences could be a consequence of the existence of several self-consistent solutions which make difficult the determination of the ground state. In contrast with the 3*d* series, there are only a few studies on 4*d* transition metal clusters. Zhao *et al.* [12] investigated the magnetic-nonmagnetic transition for elements located at the beginning of the 4*d* series. They predicted that the number of atoms required to reach the transition critical size (N_c) is surprisingly as large as 93 for Y clusters, but small for Zr, Nb, Mo, and Tc clusters ($7 < N_c < 11$). The former tendency to low magnetization has been confirmed recently by both *ab initio* [13] and semi-empirical [14] approaches. However, the reduced number of structures assumed in these calculations together with their high symmetry makes difficult to understand how the magnetic properties change when the electrons of a single atom become part of a group of several atoms and delocalize, and how bulk-like behavior is reached. Moreover, as previously stated, the existence of multiple magnetic solutions with small energy differences makes difficult the determination of the ground state solution and as a consequence it is hard to get unambiguous results for the magnetic moments.

In this paper we are particularly interested in the case of Yttrium clusters for which different theoretical calculations have obtained contradictory results. Zhang *et al.* [15] have performed *ab initio* calculations for 6-atom clusters with octahedral symmetry along the 4*d* TM series. In particular, Y_6 was found to be nonmagnetic. In the calculation of Kaiming *et al.* [13], 13-atom Yttrium clusters are considered: icosahedron (I_h), cubooctahedron (O_h), and a compact portion of the hcp lattice (D_{3h}). The binding energy differences among them are less than 0.03 eV/at, therefore it is difficult to make a definitive conclusion about the most stable structure. Contrary to these small energy differences, large discrepancies are observed for the

[a] e-mail: spanjard@lps.u-psud.fr
[b] *Full address*: Commissariat à l'Énergie Atomique, Direction des Sciences de la Matière, Département de Recherche sur l'État Condensé, les Atomes et les Molécules, Service de Recherche sur les Surfaces et l'Irradiation de la Matière, Centre d'Études de Saclay, 91191 Gif-sur-Yvette, France.

average magnetic moment $\langle M\rangle$ ($\langle M\rangle = 1\,\mu_B$/at for I_h and $\langle M\rangle = 0.23\,\mu_B$/at for O_h and D_{3h}). The former results, together with the large critical size estimated for the magnetic-nonmagnetic transition, make Y_N clusters good candidates to study the electronic and structural effects on the magnetic properties in low dimensional systems.

In transition metal clusters, it has been shown that the quasi-localized d band almost dominates the electronic and magnetic properties of the cluster, the *sp* electrons being factors of secondary importance concerning their contribution to the total moment. However, the *sp* valence orbitals can be important, mainly at the beginning of the transition metal series, for determining bond length changes on which the magnetic properties do depend, but, as we will show in this work, the average magnetic moment $\langle M\rangle$ can remain constant over large domains of distances and thus only a few different values of $\langle M\rangle$ are found for realistic distances. In this paper, we analyze the electronic and magnetic properties of small Y_N clusters as a function of the size and symmetry of the structures, by means of a tight-binding Hubbard Hamiltonian with electron-electron interactions treated in the Hartree-Fock approximation (HFA) [16]. Atomic relaxation effects are analyzed by performing calculations for several interatomic spacings. Within our model, we explore also the existence of multiple magnetic solutions by changing our initial spin-polarized electronic configuration in our self-consistent diagonalization process. These multiple magnetic solutions correspond to local minima of the total energy as a function of the magnetic moment of the system for a given geometry, among which the one that gives the lowest total energy is regarded as the ground state of the cluster and the rest with higher energies are only metastable states. The results will be compared with recent *ab initio* calculations.

The paper is organized as follows. The model Hamiltonian and its parameterization are briefly described in Section 2. In Section 3 we present our results for the magnetic properties of small Y_N clusters. Finally, the summary and conclusions are given in Section 4.

2 The model

The semiempirical model used here has been described in detail elsewhere [16], thus we only summarize its main points and discuss the choice of parameters. We adopt a tight-binding Hubbard Hamiltonian for the d band in the rotationally invariant form in orbital space [17] using the basis of $4d$ real atomic spin-orbitals $|i\lambda\sigma\rangle$ centered at each site i. The most important matrix elements of the Coulomb interaction are included: on-site interorbital (U) and intraorbital ($U + 2J$) Coulomb integrals, exchange (J) integrals, and the intersite Coulomb terms (V_{ij}). The values of U and J are actually an average over all couples $\lambda\mu$ ($\lambda \neq \mu$). This approximation has been discussed in a previous work [14] and shown to be fully justified. The electronic structure of the cluster is determined by solving this model with the interactions treated in the HFA. This leads to the following Hamiltonian [16]:

$$H_{HFA} = \sum_{i\lambda,\sigma} \epsilon_{i\lambda\sigma} n_{i\lambda\sigma} + \sum_{i,\lambda,\mu\neq\lambda,\sigma} h_{i,\lambda\mu,\sigma} a^\dagger_{i\lambda\sigma} a_{i\mu\sigma} + \sum_{i\lambda,j\mu,i\neq j,\sigma} t_{i\lambda,j\mu} a^\dagger_{i\lambda\sigma} a_{j\mu\sigma} \quad (1)$$

in the usual notations. The on-site energy levels, $\epsilon_{i\lambda\sigma}$, are functions of the spin-orbital occupation numbers $\langle n_{i\lambda\sigma}\rangle$ and electron-electron interactions. For convenience we measure them from the average value ϵ^o_d, obtained when each atom is occupied by N_a $4d$ electrons ($N_a = N_e/N$, where $N_e(N)$ is the total number of $4d$ electrons(atoms) in the cluster) and each individual orbital by $n_a = N_a/5$ electrons. Since the hybridization between the d and *sp* electrons is not explicitly included, one has to assume a particular filling of the d states. With these assumptions $\epsilon_{i\lambda\sigma}$ can be written as:

$$\begin{aligned}\epsilon_{i\lambda\sigma} = \epsilon^o_d &+ (U - \frac{1}{2}J)(N_i - N_a) \\ &- \frac{1}{2}(U - 3J)(\langle n_{i\lambda}\rangle - n_a) - \frac{1}{2}\xi_\sigma J M_i \\ &- \frac{1}{2}\xi_\sigma (U + J)\langle m_{i\lambda}\rangle + \sum_{j(i)} V_{ij}(N_j - N_a), \quad (2)\end{aligned}$$

where $\xi_\sigma = \pm 1$ for $\sigma = \uparrow, \downarrow$, and $j(i)$ stands for the neighbors of site i. Here we have introduced the orbital occupation number $\langle n_{i\lambda}\rangle = \langle n_{i\lambda\uparrow}\rangle + \langle n_{i\lambda\downarrow}\rangle$, and the magnetic moment of orbital λ $\langle m_{i\lambda}\rangle = \langle n_{i\lambda\uparrow}\rangle - \langle n_{i\lambda\downarrow}\rangle$. N_i is the total number of valence d electrons of atom i, and M_i is the magnetic moment. The quantity V_{ij} stands for the intersite Coulomb interaction assumed to be inversely proportional to the bond length R_{ij}. In the bulk $N_j = N_a$ and the last term in equation (2) vanishes. The way of calculating the effective levels is thus comparable to that used in LDA+U approach [18].

The second term in equation (1) corresponds to the intrasite interorbital Fock terms ($\bar\sigma = -\sigma$),

$$h_{i,\lambda\mu,\sigma} = -(U - J)\langle a^\dagger_{i\mu,\sigma} a_{i\lambda,\sigma}\rangle + 2J\langle a^\dagger_{i\mu,\bar\sigma} a_{i\lambda,\bar\sigma}\rangle. \quad (3)$$

They vanish in the bulk since $\langle a^\dagger_{i\lambda,\sigma} a_{i\mu,\sigma}\rangle = 0$ if $\lambda \neq \mu$ due to cubic symmetry. This is, however, not the case when the symmetry is lowered and these terms have to be included in order to conserve the actual symmetry properties of the system [16]. Finally the hopping integrals $t_{i\lambda,j\mu}$ are obtained in the Slater-Koster scheme [19] from the parameters ($dd\sigma$), ($dd\pi$) and ($dd\delta$). They are assumed to vanish beyond first nearest neighbors and to decrease exponentially with a damping exponent q [$\sim \exp(-qR_{ij})$] when the distance R_{ij} increases. We have adopted the relations $(dd\pi) = -(dd\sigma)/2$ and $(dd\delta) = 0$, and the value ($-$ 0.788 eV) of ($dd\sigma$) at the bulk interatomic spacing R_o has been fitted to the bandwidth of bulk Y derived from *ab initio* calculations.

The magnetic states of the clusters are determined by computing the the total energy given by the following equation,

$$E = \langle H_{HFA} \rangle - \langle H_{int,HFA} \rangle + E_{rep}. \quad (4)$$

The first term is the sum of the occupied one-particle energies in the HFA, while the second term is the correction due to double counting. The repulsive energy E_{rep} is described by a sum of pair interaction energies $A(R_{ij})$ between first nearest neighbors. The function $A(R_{ij})$ is of the Born-Mayer type, *i.e.*, $A(R_{ij}) = A_o \exp(-pR_{ij})$. We use the ratio $p/q = 3$ which fits [20] the universal potential energy curves of Smith *et al.* [21]. The value of pR_0 is then deduced from the experimental ratio of the bulk modulus B to the cohesive energy E_{coh}. It is well known that both quantities are underestimated in a pure d-band model but their ratio should be correctly reproduced. Finally, the value of A_0 is deduced from the equilibrium equation for the bulk.

The atomic on-site interaction U has been estimated by Van der Marel and Sawatzky [22] using spectroscopic data. In the bulk it should be reduced for two reasons: first due to screening and second to simulate the effects of electron correlations [16]. Finally we have chosen $U = 0.8$ eV irrespective of the size of the cluster. Note that this value is comparable to that used for other elements in the $4d$ series [14]. The value for the exchange interaction $J = 0.3$ eV is determined by using an empirical formula found in reference [22]. The intersite Coulomb interaction at the bulk distance $R_{ij} = R_0$ is set equal to 0.5 eV for all considered structures which is a reasonable value as discussed in [16]. The number of electrons per site will be fixed to $N_a = 2$, *i.e.*, close to the bulk configuration and in agreement with the *ab initio* calculation of Kaiming *et al.* [13] for Y_{13}^{fcc}. However, small variations around this number will be considered in some cases in order to quantify the band filling effects.

3 Results and discussion

In this section we present in Figures 1, 2, and 4 our results for the average magnetic moment of small Y_N clusters as a function of the interatomic spacing. Several types of cluster structures are considered in the calculations (see Fig. 1 of Ref. [10]). For $N = 5$ an hexahedral structure (hex) is assumed which contains atoms with coordination $z = 4$ and $z = 3$. For $N = 6$, we use a small portion of the fcc lattice (octahedron) formed by atoms with $z = 4$ as well as a trigonal (tri) arrangement ($z = 3$). Y_7 is a pentagonal dipyramid (pen). For $N = 9$, a small portion of the hcp lattice is considered as well as a structure obtained from a twisted double-square pyramid (twt) with a missing apex (Y_9^{twt}) which is reintroduced for $N = 10$ (see Fig. 1 of Ref. [23]). The Y_{13} clusters are made of a central atom surrounded by 12 first nearest neighbors arranged according to O_h, I_h and D_{3h} symmetries. They will be respectively denoted in the following as Y_{13}^{fcc} or O_hY_{13}, Y_{13}^{ico} or I_hY_{13} and Y_{13}^{hcp} or $D_{3h}Y_{13}$. The Y_{19}^{fcc} and Y_{19}^{hcp} clusters

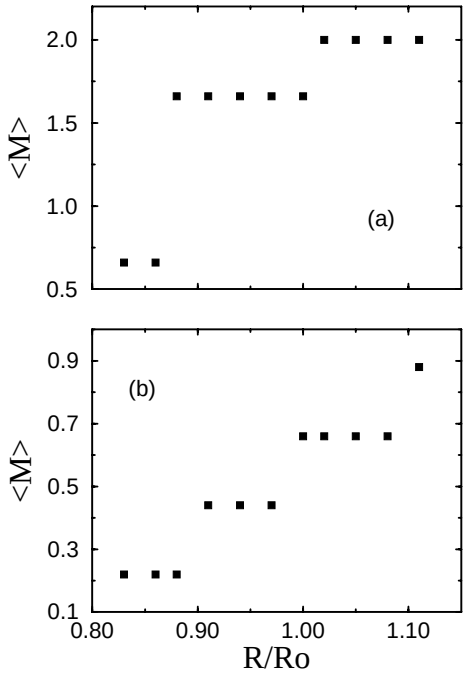

Fig. 1. The average magnetic moment per atom $\langle M \rangle$ (μ_B) as a function of the interatomic distance for (a) fcc Y_6 ($N_e = 12$) and (b) hcp Y_9 ($N_e = 18$) in the ground state.

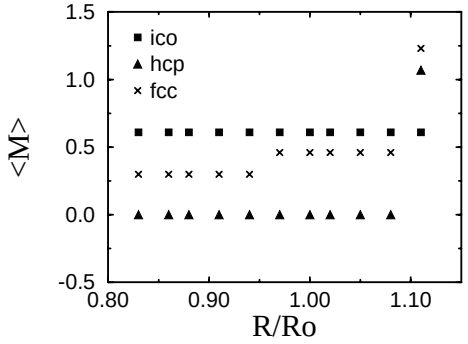

Fig. 2. The average magnetic moment per atom $\langle M \rangle$ (μ_B) as a function of the interatomic distance in Y_{13} clusters for the ground state. Results for $N_e = 26$.

are obtained respectively from Y_{13}^{fcc} and Y_{13}^{hcp} by adding 6 next nearest neighbors of the central atom.

As can be observed from the figures, the average magnetic moment takes only a reduced set of values and can be considered as almost constant over large regions of variations in the interatomic spacing for most of the clusters. Several magnetic solutions are found for each value of R/R_o, being close in energy and having different values for the total moment. The data reported in Figures 1, 2, and 4 give the solution with the lowest total energy which is regarded as the ground state. Note that at large bond distances, high values of $\langle M \rangle$ are obtained in all cases which is a consequence of the high degree of localization of the d electrons, but, as the interatomic distance

is reduced, the average magnetic moment decreases in a stepwise manner with rather wide steps. For example, in octahedral Y_6 the average magnetic moment remains equal to $1.66\,\mu_B$/at when R varies between R_o and $0.9R_o$, *i.e.*, for realistic variations in the interatomic distance. This value is much larger that the one given in the *ab initio* calculation of Zhang *et al.* [15] in which the O_hY_6 cluster was found to be nonmagnetic. This large difference could be due to the existence of multiple magnetic solutions in both theoretical approaches. However, it is important to note that in our model we have checked all the possible initial configurations for spin-up and spin-down electrons when starting the self-consistent iteration process. Actually, the nonmagnetic state was always present for all the interatomic spacings but it was energetically less stable than the magnetic solutions. Moreover, for such small sizes the low coordination number of the atoms together with the high symmetry of the cluster usually favor a nonzero magnetization.

For the hcp Y_9 cluster, the magnetic properties are more sensitive to the bond length (Fig. 1b). Moreover, several metastable solutions close in energy are present. At the bulk interatomic bond length R_o, we obtain $\langle M\rangle = 0.66\,\mu_B$/at but small contractions change the value of $\langle M\rangle$ to $0.44\,\mu_B$/at and this last solution becomes the most stable over a domain of 8% of reduction in the distance. The magnetic order within the Y_9 cluster is found to be antiferromagnetic in all the steps present in the figure, the sign of the magnetic moment ($\downarrow$) of the most coordinated site being opposite to that ($\uparrow$) of the other sites. Ferromagnetic (F) and nonmagnetic solutions are also present but as metastable states. In this structure as in the rest of the clusters, the most coordinated atoms have the largest excess of electrons, since their local density of states (LDOS) has the largest width. These electrons are mainly of spin-down character, a fact that favors the antiferromagnetic alignment in the cluster.

As discussed in a previous work [23], the actual change in $\langle M\rangle$ at each step shown in Figure 1 is determined by the degeneracy and spacing of the one-electron energy levels around the Fermi level E_F. Small energy differences between the highest occupied molecular orbital (HOMO) and the lowest unoccupied molecular orbital (LUMO) can very easily allow level inversions when the interatomic distance is varied and this could lead to a change in the cluster moment. The strongly symmetric O_hY_6 cluster that has a highly degenerate one-particle energy spectrum with large level spacings, does not allow for easy modifications in the order of the HOMO and the LUMO levels and, as a consequence, a small number of magnetic solutions are observed as the bond length is reduced. Contrary to this result, in the hcp Y_9 cluster which is less symmetric, a larger number of steps are observed which illustrates the general trend that less symmetric geometries are more flexible as concerns the magnetic solutions due to their lower degeneracies of the electronic levels. However, as we will see in the following, band filling effects may play also a fundamental role in the existence of different magnetic states, since small variations in the number of d electrons could lead to new closed or open shell electronic configurations in the clusters which are known to change the stability of the magnetic solutions.

In Figure 2, 13-atom clusters are considered: icosahedral (I_h), cuboctahedral (O_h), and a compact portion of the hcp lattice. Remarkably, the I_h cluster is able to maintain the solution $\langle M\rangle = 0.61\,\mu_B$/at over the range of R/R_o spanned in the figure. As in previous cases, this behavior can be explained by analyzing the one-electron energy levels of the cluster, as shown in Figure 1 of reference [14]. In our calculation, the configuration $N_\uparrow = 17$ and $N_\downarrow = 9$ corresponds to a closed shell electronic configuration for both spin directions, a solution which is expected to be quite stable against modifications in the interatomic distance. Moreover, large energy differences are obtained between the electronic levels which anticipates a reduced number of steps for $\langle M\rangle$ as the interatomic distance is varied. Our calculated average magnetic moment for this cluster is smaller than the one given in the *ab initio* calculation of Kaiming *et al.* [13] ($\langle M\rangle = 1\,\mu_B$/at) for the same structure, however as we will see in the following, the same trend is observed concerning its magnitude as compared with the other two isomers ($\langle M\rangle(ico) > \langle M\rangle$(fcc,hcp)). The average magnetic moment for the O_h cluster is more sensitive to the interatomic spacing. On comparing with the calculation of Kaiming *et al.* for the O_hY_{13} cluster ($\langle M\rangle = 0.24\,\mu_B$/at) we observe that our result for $\langle M\rangle$ at the bulk equilibrium spacing ($\langle M\rangle = 0.46\,\mu_B$/at) is larger, but as we can see from the figure a contraction of approximately 5% in the distance can reduce the average magnetic moment to $0.3\,\mu_B$/at a value which is in good agreement with the *ab initio* result. Finally, in the hcp cluster $\langle M\rangle = 1.07\,\mu_B$/at is obtained for large interatomic spacings (10% of expansion), however, small contractions from this value makes the nonmagnetic state the most stable solution. In the three considered structures, the antiferromagnetic alignment of the local moments is preferred save for the O_h geometry in which a ferromagnetic configuration is the most stable solution in the range of approximately $1.0 < R/R_o < 1.05$. This can be seen from Figure 3 where we show the behavior of the local moments and the local charges for the fcc Y_{13} cluster as a function of the bond length. In Figure 3a, we observe that $\langle M\rangle$ (see Fig. 2) follows the same behavior as the local moment of the atoms located at the surface of the cluster, from which the dominant contribution to the total magnetization is obtained. Note that the variation of the local moment on the central atom is more subtle since the small oscillation that is present is able to change the magnetic order within the structure from AF to F and then AF again. As we observe from Figure 3b, where we plot the spin-polarized charge distribution as a function of the interatomic distance, the behavior of the local moments follows from the redistribution of the local charge. As stated before, we observe that the most coordinated atom has the largest number of $4d$ electrons mainly of spin-down character, a fact that favors the antiferromagnetic alignment of the local moments.

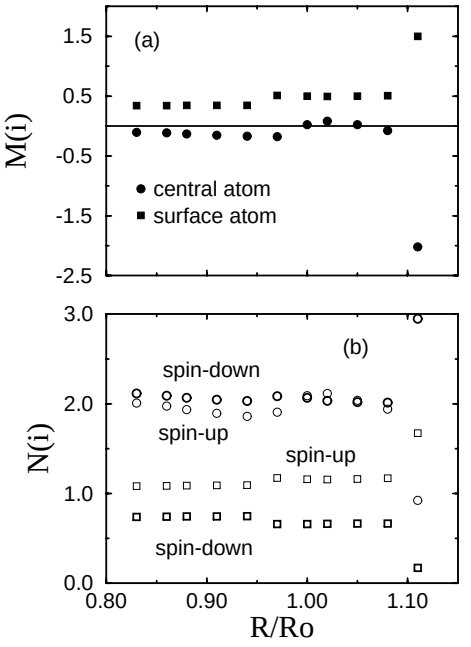

Fig. 3. (a) The local magnetic moments $M(i)$ (μ_B) and (b) the spin-polarized charge distribution as a function of the interatomic distance for the fcc Y_{13} cluster in the ground state. The circles refer to the central atom and the squares to surface atoms. Results for $N_e = 26$.

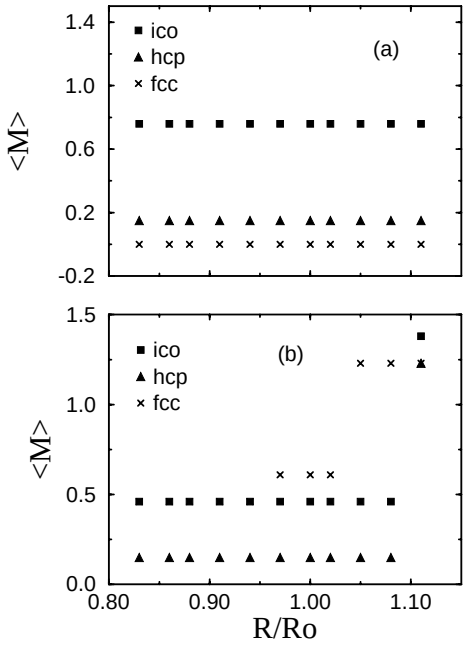

Fig. 5. The average magnetic moment per atom $\langle M \rangle$ (μ_B) as a function of the interatomic distance for Y_{13} clusters in the ground state for two values of the total number of electrons N_e: (a) $N_e = 24$, (b) $N_e = 28$.

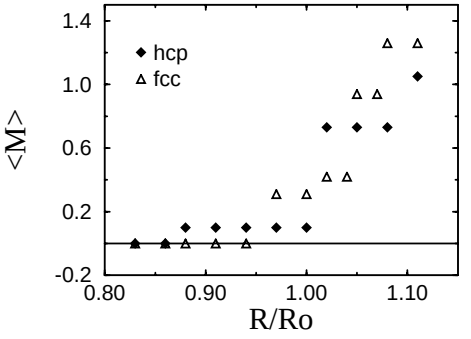

Fig. 4. The average magnetic moment per atom $\langle M \rangle$ (μ_B) as a function of the interatomic distance for a fcc and a hcp Y_{19} cluster in the ground state. Results for $N_e = 38$.

In Figure 4, 19-atom clusters are considered having fcc and hcp symmetries. Note that a larger number of magnetic states are obtained in the fcc geometry, which reveals that small energy differences are obtained between the electronic levels around E_F. In the Y_{19}^{fcc} cluster, a contraction of approximately 5% relative to the bulk bond length favors the stability of the nonmagnetic state over the magnetic solutions. At large distances a ferromagnetic solution is obtained ($\langle M \rangle = 1.26\,\mu_B$/at), however as the interatomic distance is reduced the antiferromagnetic configuration ($\downarrow\uparrow\uparrow$) becomes the most stable one, a fact that obviously favors the tendency to the zero net magnetization. The Y_{19}^{hcp} cluster reaches the nonmagnetic state for approximately a contraction of 12%. In this case for realistic variations in the interatomic distance (5% of contraction) the average magnetic moment remains constant and equal to $0.1\,\mu_B$/at. Such a behavior is in contrast with the one found for the local moments for which both ferromagnetic and antiferromagnetic configurations are obtained in the range of $0.88 < R/R_o < 1.0$. It is important to note that in all magnetic solutions a closed electronic shell is obtained for at least one spin direction. Moreover, partially closed shell solutions are generally less stable than those having a closed shell configuration for both spin directions. However in some cases, the energy gain upon magnetization can overcome this general trend.

In order to see the effects of the d band filling on the magnetic properties, we have performed calculations for 13-atom O_h, I_h, and D_{3h} clusters for $N_e = 24$ and 28 as a function of the bond length. As stated before, small variations in the number of electrons in the system could change the nature of the HOMO from an open to a closed shell (or *vice versa*) electronic configuration and as a consequence new magnetic states could arise. As we can see from Figures 2 and 5, the influence of the d band filling is more important for the $O_h Y_{13}$ as compared to the I_h and hcp geometries. Here, the change in the position of the HOMO and the details of the energy-level distribution play a major role. This fact is clearly seen from Figure 5 where different band fillings lead to significant changes in the position and extension of the steps as well as in the magnitude of the total moment in the O_h cluster. Contrary to this result the I_h and hcp geometries have almost the same magnetic structure and only small variations

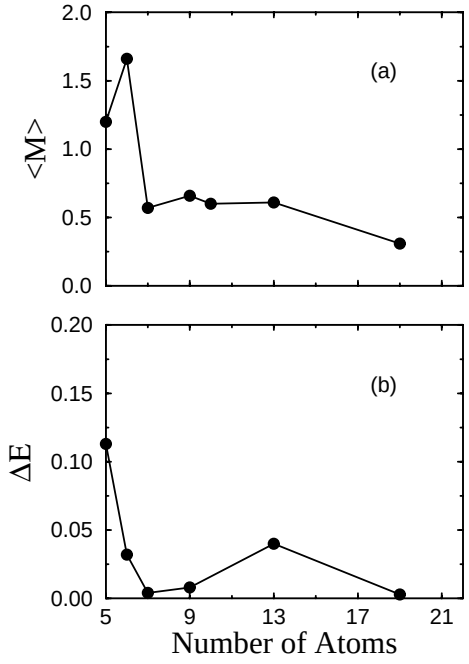

Fig. 6. (a) The average magnetic moment per atom $\langle M\rangle$ (μ_B) and (b) the magnetic energy gain upon magnetization ΔE (eV/at) as a function of the cluster size for the most stable structures at the bulk interatomic spacing. Results for $N_a = 2$.

of $\langle M\rangle$ are present, as compared to the results with $N_e = 26$. Moreover, as we can see also from Figure 5b, band filling effects can overcome the usual symmetry rules since less symmetric structures can have larger average magnetic moments ($\langle M\rangle(O_h) > \langle M\rangle(I_h)$) for a given N_e. A similar result has been found by Jinlong *et al.* [24] in the case of Rh_{13} clusters.

In Table 1 we present the results for the total binding energy E, the average magnetic moment per atom $\langle M\rangle$, and the local magnetic moments $M(i)$ for each type of site in the clusters at the bulk interatomic spacing. For some cluster sizes, different structures are considered in order to see the effect of the local environment on the magnetic properties. As can be observed from the Table, the existence of metastable magnetic states is seen in almost all the considered structures. Ferromagnetic as well as antiferromagnetic configurations are present, the latter being stabilized mainly for the larger sizes which obviously favors the tendency to a net zero magnetization. Note that small energy differences are obtained between isomers while the magnetic properties differ considerably. On comparing with the *ab initio* results for $O_h Y_6$ and O_h and $I_h Y_{13}$, we can see that our calculated binding energy is underestimated since we do not take explicitly into account the contributions of the *sp* electrons in our model. Note that $\langle M\rangle = 0$ for the hcp Y_{13} and $\langle M\rangle = 0.1\,\mu_B$/at for the hcp Y_{19} which indicates that a bulk-like configuration with the bulk bond length tends to suppress magnetism.

Concerning the distribution of the local magnetic moments, we can see from Table 1 that the less coordinated

Table 1. The calculated energy per atom E (eV), the average magnetic moment per atom $\langle M\rangle$ (μ_B/at), and the local magnetic moment per atom $M(i)$ (μ_B/at) for small Y_N clusters at the bulk interatomic spacing. The type i of sites in the clusters have been ordered according to their coordination in ascending order. Results for $N_a = 2.0$.

CLUSTER	$E(N)$	$\langle M\rangle$	$M(1)$	$M(2)$	$M(3)$	$M(4)$
Y_5^{hex}	10.04	1.20	1.18	1.23		
Y_5^{hex}	9.68	0.40	0.66	0.00		
Y_5^{hex}	9.47	0.00	0.00	0.00		
Y_6^{fcc}	11.52	1.66	1.66			
Y_6^{fcc}	11.33	0.00	0.00			
Y_6^{tri}	10.56	0.33	0.33			
Y_7^{pen}	14.68	0.57	0.93	0.42		
Y_7^{pen}	14.65	0.85	0.80	0.87		
Y_7^{pen}	14.64	0.00	0.00	0.00		
Y_9^{hcp}	19.57	0.66	−0.81	1.52	0.66	0.61
Y_9^{hcp}	19.55	0.23	−0.10	0.42	0.05	0.28
Y_9^{hcp}	19.49	0.00	0.00	0.00	0.00	0.00
Y_9^{twt}	19.10	0.22	0.51	−0.01	−0.01	
Y_9^{twt}	19.03	0.44	0.76	0.11	0.20	
Y_9^{twt}	19.01	0.00	0.00	0.00	0.00	
Y_{10}^{twt}	21.18	0.60	0.63	0.47		
Y_{13}^{ico}	30.80	0.61	−0.49	0.70		
Y_{13}^{ico}	30.17	0.00	0.00	0.00		
Y_{13}^{hcp}	29.76	0.00	0.00	0.00	0.00	
Y_{13}^{hcp}	29.64	0.30	−0.02	0.11	0.56	
Y_{13}^{fcc}	29.33	0.46	0.02	0.50		
Y_{13}^{fcc}	29.30	0.00	0.00	0.00		
Y_{13}^{fcc}	29.27	0.15	−0.05	0.17		
Y_{19}^{fcc}	46.17	0.31	−0.01	0.47	0.05	
Y_{19}^{fcc}	46.11	0.00	0.00	0.00	0.00	
Y_{19}^{hcp}	45.27	0.10	−0.06	0.20	0.09	0.05
Y_{19}^{hcp}	44.53	0.21	0.04	0.16	0.31	0.17
Y_{19}^{hcp}	44.52	0.52	0.84	0.50	0.44	0.58

Table 2. The spin magnetic moment $2\langle S_z\rangle$, the orbital magnetic moment $\langle L_z\rangle$, and the total magnetic moment $2\langle S_z\rangle + \langle L_z\rangle$ in Bohr magnetons. Results are given for $N_a = 2.0$. The z-direction is one of the fivefold symmetry axis in Y_{13}^{ico}, the c-axis in Y_{13}^{hcp} and one of the cubic axes for Y_{13}^{fcc}.

CLUSTER	$2\langle S_z\rangle$	$\langle L_z\rangle$	$2\langle S_z\rangle + \langle L_z\rangle$
Y_{13}^{ico}	0.611	−0.023	0.588
Y_{13}^{hcp}	0.304	−0.011	0.292
Y_{13}^{fcc}	0.000	0.000	0.000

atoms do not always have the largest $M(i)$. For example, for the Y_7^{pen} in the ground state solution, the two atoms with coordination $z = 5$ have a local moment $M(1) = 0.93\,\mu_B$/at while $M(2) = 0.42\,\mu_B$/at for the five atoms with $z = 4$. However, note that the metastable magnetic solution for the same cluster follows the expected behavior for $M(i)$. In this context, it is important to point out that all the possible initial configurations for spin-up and spin-down electrons have been considered when starting the self-consistent diagonalization process. From Table 1 and Figure 6 we can see that the average magnetic moment reveals a remarkable size and structural dependence which seems to be characteristic of systems showing unsaturated itinerant magnetism. For $N = 5$ and $N = 6$ (see Fig. 6a), large values of $\langle M\rangle$ are obtained for the most stable structures at the bulk equilibrium distance. For $N = 7$, $\langle M\rangle$ decreases abruptly and remains almost constant ($\langle M\rangle \approx 0.6\,\mu_B$/at) until $N = 13$, then it decreases slowly. In Figure 6b, we show the energy gain upon magnetization ΔE ($\Delta E = E(\langle M\rangle = 0) - E(\langle M\rangle)$) as a function of the cluster size for the most stable structures at $R/R_o = 1$. It is seen that Y_N clusters could be magnetic up to five atoms, but for larger sizes magnetic and nonmagnetic states may be equally probable due to their small energy differences. Moreover, small deviations from the highly symmetric structures considered in this calculation can change the total moment of the cluster and as a consequence the low-spin states could arise as the new ground state in the structures. These small energy gains upon magnetization should be compared with the ones found in Rh_N clusters for which recent experimental studies have found a nonzero magnetization. For example, for the I_hY_{13} cluster at the equilibrium bulk distance $\Delta E = 0.04$ eV/at, while for I_hRh_{13} we obtain with the same model $\Delta E = 0.31$ eV/at. The former result gives some support to our predicted tendency to low magnetization state in this kind of systems.

As stated previously, the energy differences between some geometrical or magnetic structures are rather small and thus can be of the order of the spin-orbit coupling parameter ξ_{SO}, which is about 0.03 eV for Y. Therefore we have checked the influence of the spin-orbit coupling on the binding energies and magnetic moments using a simplified Hamiltonian. In this Hamiltonian, which has been described elsewhere [25], the on-site energy levels are renormalized only by the total charges and magnetic moments on each site. In addition, the spin-orbit coupling term $\xi_{SO}(\mathbf{L}.\mathbf{S})$ is assumed to have only intra-atomic matrix elements as usual in the tight-binding approximation [26]. The calculations have been carried out for Y_{13}^{ico}, Y_{13}^{fcc} and Y_{13}^{hcp}. The change of binding energy due to the spin-orbit coupling is of the order of 10^{-3} eV per atom for the three structures. Finally, the corresponding results for the magnetic moments are given in Table 2. We can see that the sign of the orbital moment is opposite to that of the spin moment, as expected for an element belonging to the first half of the TM series, but the effect is very small. Consequently, the spin-orbit coupling should not modify the trends put forward in this work.

4 Summary and conclusions

We have presented the results of self-consistent calculations for the electronic and magnetic properties of small Y_N clusters, using realistic tight binding parameters. The magnetic states in the clusters are found to be determined by the details of the local environment together with the strong sensitivity of the electronic structure around E_F to the size and symmetry of the clusters. The behavior of the average magnetic moment as a function of the cluster size is nonmonotonic which seems to be characteristic of nonsaturated magnetic systems.

The main advantage of the considered tight-binding model is its simplicity which allowed us to get a physical insight into the nature of the magnetic properties of small Y_N clusters. These studies are complementary to the existing *ab initio* calculations since we have concentrated here rather on qualitative trends than on accurate description of the systems.

The authors would like to thank Professor J. Dorantes-Dávila and Professor G. Pastor for stimulating discussions. One of us (RGL) would like to acknowledge the hospitality of the Service de Recherche sur les Surfaces et l'Irradiation de la Matière of Centre d'Études de Saclay where part of the calculation has been made as well as the financial support by CONACyT, Mexico.

References

1. W.A. deHeer, P. Milani, A. Chatelain, Phys. Rev. Lett. **65**, 488 (1990).
2. D.C. Douglass, J.P. Bucher, L.A. Bloomfield, Phys. Rev. B **45**, 6341 (1992).
3. J.G. Louderback, A.J. Cox, L.J. Lising, D.C. Douglas, L.A. Bloomfield, Z. Phys. D **26**, 301 (1993).
4. G.M. Pastor, J. Dorantes-Dávila, K.H. Bennemann, Phys. Rev. B **40**, 7642 (1989).

5. F. Liu, S.N. Khanna, P. Jena, Phys. Rev. B **43**, 8179 (1991).
6. K. Lee, J. Callaway, S. Dhar, Phys. Rev. B **30**, 1724 (1985).
7. K. Lee, J. Callaway, Phys. Rev. B **48**, 15358 (1993).
8. A.J. Cox, J.G. Louderback, S.E. Apsel, L.A. Bloomfield, Phys. Rev. B **49**, 12295 (1994).
9. D. Kaiming, Y. Jinlong, X. Chuamyun, W. Kelin, Phys. Rev. B **54**, 2191 (1996).
10. R. Guirado-López, D. Spanjaard, M.C. Desjonquères, F. Aguilera-Granja, J. Magn. Magn. Mater. **186**, 214 (1998).
11. B.V. Reddy, S.N. Khanna, B.I. Dunlap, Phys. Rev. Lett. **70**, 3323 (1993).
12. J. Zhao, X. Chen, Q. Sun, G. Wang, Europhys. Lett. **32**, 113 (1995).
13. D. Kaiming, Y. Jinlong, X. Chuamyun, W. Kelin, Phys. Rev. B **54**, 11097 (1996).
14. R. Guirado-López, D. Spanjaard, M.C. Desjonquères, A.M. Olés, Europ. Phys. Jour. B **3**, 437 (1998).
15. G.W. Zhang, Y.P. Feng, C.K. Ong, Phys. Rev. B **54**, 17208 (1996).
16. B. Piveteau, M.C. Desjonquères, A.M. Oleś, D. Spanjaard, Phys. Rev. B **53**, 9251 (1996).
17. A.M. Oleś, Phys. Rev. B **28**, 327 (1983).
18. V.I. Anisimov, J. Zaanen, O.K. Andersen, Phys. Rev. B **44**, 943 (1991).
19. J.C. Slater, G.F. Koster, Phys. Rev. **94**, 1498 (1954).
20. D. Spanjaard, M.C. Desjonquères, Phys. Rev. B **30**, 4822 (1984).
21. J.R. Smith, J. Ferrante, J.H. Rose, Phys. Rev. B **25**, 1419 (1982).
22. D. van der Marel, G.A. Sawatzky, Phys. Rev. B **37**, 10674 (1988).
23. Y. Jinlong, F. Toigo, W. Kelin, Phys. Rev. B **50**, 7915 (1994).
24. Y. Jinlong, F. Toigo, W. Kelin, Z. Manhong, Phys. Rev. B **50**, 7173 (1994).
25. G.M. Pastor, J. Dorantes-Dávila, S. Pick, H. Dreyssé, Phys. Rev. Lett. **75**, 326 (1995).
26. J. Friedel, P. Lenglart, G. Leman, J. Phys. Chem. Solids **25**, 781 (1964).